

This discussion paper is/has been under review for the journal Atmospheric Measurement Techniques (AMT). Please refer to the corresponding final paper in AMT if available.

**Aerosol impact on
the NO₂ airmass
factor**

J. Leitão et al.

On the improvement of NO₂ satellite retrievals – aerosol impact on the airmass factors

**J. Leitão¹, A. Richter¹, M. Vrekoussis¹, A. Kokhanovsky¹, Q. J. Zhang²,
M. Beekmann², and J. P. Burrows¹**

¹Institute of Environmental Physics, University of Bremen, Bremen, Germany

²Laboratoire Inter-Universitaire des Systèmes Atmosphériques (LISA), CNRS et Universités Paris 12 et Paris 7, Créteil, France

Received: 18 November 2009 – Accepted: 19 November 2009

– Published: 11 December 2009

Correspondence to: J. Leitão (jleitao@iup.physik.uni-bremen.de)

Published by Copernicus Publications on behalf of the European Geosciences Union.

Title Page

Abstract

Introduction

Conclusions

References

Tables

Figures

◀

▶

◀

▶

Back

Close

Full Screen / Esc

Printer-friendly Version

Interactive Discussion



Abstract

The accurate determination of nitrogen dioxide (NO_2) tropospheric vertical columns from satellite measurements depends, partly, on the airmass factor (AMF) used. A sensitivity study was performed with the radiative transfer model SCIATRAN to better understand the impact of aerosols in the calculation of NO_2 AMFs. This influence was studied by varying the NO_2 and aerosol vertical distributions, as well as physical and optical properties of the particles. The key factors for these calculations were identified as the relation between trace gas and aerosol vertical profiles, the optical depth of the aerosol layer, and single scattering albedo. Overall it was found that aerosol mixed with the trace gas increases the measurements' sensitivity. The largest change, a factor of ~ 2 relative to the situation without aerosols, was found when a low layer of aerosol (600 m) was combined with a homogenous NO_2 layer of 1.0 km. A layer of aerosol above the NO_2 will usually reduce the sensitivity of the satellite measurement, a situation found mostly for runs with discrete elevated aerosol layers representative for long-range transport of aerosols that can generate a decrease of the AMF values of up to 70%. The use of measured aerosol profiles and modelled NO_2 resulted, generally, in a much smaller changes of AMF relative to the pure Rayleigh case. Exceptions are some events of elevated layers with high aerosol optical depth that lead to a strong decrease of the AMF values. These results highlight the importance of aerosols in the retrieval of tropospheric NO_2 columns from space and indicate the need for detailed information on aerosol properties and vertical distribution.

1 Introduction

The possibility of measuring trace gases (e.g. ozone (O_3), nitrogen dioxide (NO_2), sulphur dioxide (SO_2), among others) from space provides a unique opportunity to observe the Earth and its atmosphere from above and, consequently, monitor the air quality in remote places with low density of in-situ measurements. Remote sensing of

Aerosol impact on the NO_2 airmass factor

J. Leitão et al.

Title Page

Abstract

Introduction

Conclusions

References

Tables

Figures

◀

▶

◀

▶

Back

Close

Full Screen / Esc

Printer-friendly Version

Interactive Discussion



atmospheric pollution is currently performed by several instruments flying on satellites. One common technique is the use of backscattered solar radiation from which information can be retrieved on the amounts of aerosols and trace gases in the atmosphere. Some instruments were mainly developed for trace gas observations, as it is the case for GOME (Burrows et al., 1999) flying on ERS-2, SCIAMACHY (Burrows et al., 1995; Bovensmann et al., 1999) on the ENVISAT platform, OMI (Levelt et al., 2006) on EOS-AURA and more recently GOME-2 (Callies et al., 2000) launched on MetOp-A. These also provide interesting information on aerosols albeit at low spatial resolution. Other instruments such as MODIS (King et al., 1992) flying on Terra and Aqua, MISR (Diner et al., 1998) also on Terra measuring with multi-angle viewpoint, or MERIS (Bézy et al., 2000) on the ENVISAT platform, are better suited for aerosol retrievals since they provide high spatial resolution and, in some cases, multiple viewing directions. More recently, the active lidar system CALIOP (Winker et al., 2003) flying on the CALIPSO satellite has become available which for the first time can resolve aerosol vertical distributions with high resolution.

Nitrogen oxides ($\text{NO}_x = \text{NO} + \text{NO}_2$) can be considered one of the main pollutants emitted in urban and industrialized areas mainly in fossil fuel combustion processes. NO_x play a key role in the basic tropospheric chemistry acting as a precursor for photochemical ozone production and acidification of the atmosphere via nitric acid (Seinfeld and Pandis, 1998). Furthermore, they also contribute to global climate change by interfering, directly and indirectly, with the Earth's radiative budget (Solomon et al., 1999; IPCC, 2007; Vasilkov et al., 2009). According to the recent Fourth Assessment Report (AR4, IPCC, 2007 and references therein) the main anthropogenic sources of NO_x include fossil fuel combustion and industrial processes followed by biomass burning. NO_x is also emitted via natural processes mostly during lightning events and as result of microbial processes in soils. As a consequence of civilization's progress and also population growth the NO_x emissions have increased drastically since preindustrial times (IPCC, 2007). While emissions in some industrialized countries have decreased over the last decade in response to emission reduction measures and use of cleaner fuels,

**Aerosol impact on
the NO_2 air mass
factor**J. Leitão et al.

[Title Page](#)[Abstract](#)[Introduction](#)[Conclusions](#)[References](#)[Tables](#)[Figures](#)[⏪](#)[⏩](#)[◀](#)[▶](#)[Back](#)[Close](#)[Full Screen / Esc](#)[Printer-friendly Version](#)[Interactive Discussion](#)

emissions in the rapidly developing economies in Asia are expected to continue their increase. In the mid-1990s NO_x emission rates for Asia were reported by Akimoto (2003) to exceed the amount emitted in North America and Europe, and in 2005, Richter et al. found a high enhancement of NO_2 columns over China measured by GOME and SCIAMACHY. This continuous trend was illustrated in the latest AR4 report and various recent publications (e.g. Zhang et al., 2007; van der A et al., 2008) where the increase in NO_x emissions is identified as being mostly related to the economical development of the country and consequential growing number of power plants. Furthermore, massive use of fertilizers and intensification of agricultural practices were also significant factors in this process. While the global budget of anthropogenic sources is relatively well constrained, the natural emissions are still rather uncertain. The most common methods to estimate NO_x emissions are “bottom-up” inventories. More recently, a “top-down” approach using NO_2 satellite measurements to estimate global or regional emissions has been used in several studies, namely using inverse modelling strategies (e.g. Martin et al., 2003; Beirle et al., 2004; Konovalov et al., 2006, 2008; van der A et al., 2008 and references therein). The satellite datasets offer advantages both on the time and spatial scales with a continuous global coverage that can often be achieved with high temporal resolution (approx. 1 to 6 days depending on the instrument coverage).

Although a great fraction of aerosols is part of the natural components of the Earth’s atmosphere, they can still be harmful for human health and contribute to visibility degradation when present in high amounts (Chang et al., 2009 and references therein; Wang et al., 2009). In addition to their relevance as pollutants, they play a major role in climate change by their direct and indirect impact on radiative forcing (e.g. IPCC, 2007). Aerosols vary strongly in size and composition, and their proper characterization, in particular using remote sensing, is still a challenge. In recent years numerous experimental studies focused on aerosols. Still, the formation processes, transport and transformation of aerosols are not completely understood. Their high spatial and temporal variability (especially for tropospheric aerosol) represents a complication to the process of identifying and quantifying its sources and types.

**Aerosol impact on
the NO_2 airmass
factor**

J. Leitão et al.

[Title Page](#)[Abstract](#)[Introduction](#)[Conclusions](#)[References](#)[Tables](#)[Figures](#)[◀](#)[▶](#)[◀](#)[▶](#)[Back](#)[Close](#)[Full Screen / Esc](#)[Printer-friendly Version](#)[Interactive Discussion](#)

**Aerosol impact on
the NO₂ airmass
factor**

J. Leitão et al.

[Title Page](#)[Abstract](#)[Introduction](#)[Conclusions](#)[References](#)[Tables](#)[Figures](#)[⏪](#)[⏩](#)[◀](#)[▶](#)[Back](#)[Close](#)[Full Screen / Esc](#)[Printer-friendly Version](#)[Interactive Discussion](#)

Aerosol present in the atmosphere interacts with radiation consequently influencing the remote sensing measurements of atmospheric trace gases. Depending on the particles' optical properties, the amount of aerosol and its vertical distribution relative to that of the trace gas of interest, the sensitivity of the satellite measurements can either be increased or decreased. As the anthropogenic sources of aerosols and other pollutants are often collocated, a proper characterization of the aerosols' impact on the retrieval is needed to accurately quantify trace gas amounts derived from satellite observations. This is of particular importance if long-term trends of, for example, tropospheric NO₂ are studied which are accompanied by large changes also in the aerosol loading.

This study assesses the importance of aerosol for the retrieval of tropospheric NO₂ columns from satellite observations. To this end, a number of different scenarios was defined with varying aerosol settings and NO₂ distributions. They were used for radiative transfer calculations with the SCIATRAN model (Rozanov et al., 2005) in order to evaluate changes in the measurements' sensitivity relative to a scenario without aerosols. The results show to which parameters the measurements are most sensitive and to which extent the modification of aerosol properties affects the results. As far we are aware, a comprehensive study as ours has not been conducted before.

The paper starts with a brief discussion of aerosol effects on radiative transfer followed by a short description of the satellite retrieval. The selection process of data used and definition of the case scenarios considered is presented in Sect. 2 together with some initial findings. The next section focuses on the results of the sensitivity study, presenting the variations of NO₂ airmass factors in response to changes in the boundary layer height, variation in the aerosol layer distribution and use of different single scattering albedo values. General conclusions are presented in the final section of this manuscript.

1.1 The effect of aerosols on the radiative transfer

Aerosols in the atmosphere interact with electromagnetic radiation both by scattering and by absorbing light. The scattering efficiency of aerosols strongly depends on their concentration, size and shape, as well as on their refractive index, determined by their chemical composition. Aerosol scattering also depends on the scattering angle and usually has a pronounced maximum for forward scattering. The details of the angular distribution of the phase function vary with the aerosol composition and the size of the particles relative to the wavelength of the radiation and also depend on particle shape and internal structure. The absorbing properties of aerosols are usually expressed via the single scattering albedo (SSA) which is defined as the ratio of scattering to extinction and depends on particle composition. For remote sensing applications, the total amount of aerosols present in the atmosphere is often specified by an aerosol optical depth (AOD) which is the vertical integral of the extinction by aerosols from the top of the atmosphere to the ground. Both the AOD and the SSA depend on wavelength.

Satellite measurements of tropospheric trace gases using scattered solar light are based on detection of the absorption along the light path from the sun through the atmosphere to the instrument. As scattering is a statistical process, many different light paths contribute to the signal observed at the top of the atmosphere. The overall absorption signal is to a first approximation determined by the amount of absorption along the individual light paths weighted with their relative contributions to the total radiance measured. Aerosols in the atmosphere can change both, the individual light path lengths and their contributions to total radiance observed at the satellite.

Qualitatively, the effects of an aerosol layer on tropospheric measurements using scattered sun light can be separated into four groups:

- Light path enhancement within the aerosol layer as result of multiple scattering, leading to an increase in absorption signal from the path between scattering events;

Aerosol impact on the NO₂ airmass factor

J. Leitão et al.

Title Page

Abstract

Introduction

Conclusions

References

Tables

Figures

◀

▶

◀

▶

Back

Close

Full Screen / Esc

Printer-friendly Version

Interactive Discussion



- Increased sensitivity within and above the aerosol layer as result of larger scattering probability and therefore a larger contributions of these paths to the radiance observed at the satellite (albedo effect);
- Decreased sensitivity below the aerosol layer as more photons are scattered back to the satellite before they can reach these altitudes (shielding effect);
- Decreased sensitivity within and below the aerosol layer in cases of strongly absorbing aerosols as the number of photons returning from this region is reduced.

One way of expressing the sensitivity of the measurement is to calculate the air mass factor (AMF) which is defined as the ratio between the apparent (slant) column of the absorber retrieved from a measurement and the vertical atmospheric column (see next section). The larger the air mass factor, the higher the sensitivity of the measurement. The aerosol effects discussed above are illustrated in Fig. 1 where the NO₂ air mass factor is shown as function of altitude for three different scenarios, highlighting the increased sensitivity in the presence of aerosols in the upper part of the layer and above it as well as the reduced sensitivity close to the surface. With the exception of the last point, the effects of aerosols listed above are very similar to the considerations made for clouds (e.g. Hild et al., 2002; Beirle et al., 2009; Kokhanovsky and Rozanov, 2009). The overall impact of aerosols on a measurement will depend on the relative importance of the 4 effects which depends on aerosol properties, aerosol amounts, surface reflectance and the vertical distribution of aerosol and trace gas of interest. The results can be both, an increase or a decrease in observed absorption signal depending on the specific conditions.

1.2 Satellite retrieval

The retrieval of tropospheric NO₂ columns from space is performed in several steps. First, NO₂ slant column densities (SC) are retrieved with the DOAS (Differential Optical Absorption Spectroscopy) technique (Platt and Stutz, 2008) in the UV/visible wavelength range. The SC corresponds to the amount of absorber present along the average light path through the atmosphere to the satellite sensor. The tropospheric SC is

Aerosol impact on the NO₂ air mass factor

J. Leitão et al.

Title Page

Abstract

Introduction

Conclusions

References

Tables

Figures

◀

▶

◀

▶

Back

Close

Full Screen / Esc

Printer-friendly Version

Interactive Discussion



calculated by eliminating the stratospheric contribution from the total columns retrieved (further details regarding the retrieval can be found, for example in Leue et al. (2001), Richter and Burrows (2002), Martin et al. (2002) and Boersma et al. (2004)). When dividing this tropospheric SC by an airmass factor (AMF) a NO₂ tropospheric vertical column density (VC) is obtained. Therefore, the AMF concept can be interpreted as the relation between the optical path through the atmosphere and the vertical optical path in the layer of interest (Solomon et al., 1987). This AMF is computed using radiative transfer calculations that require information on measurement conditions (such as, observation geometry and wavelength) and atmospheric characteristics (e.g. vertical distribution of the chemical species, surface albedo, aerosol loading and clouds). Hence, an appropriate selection of the a priori assumptions used is essential to obtain the correct values of the AMF and thus the NO₂ VC. In the event of selecting an AMF that is too high, the resulting VC will be underestimated. Likewise, the determined NO₂ VC will be too large if the value of the AMF used for the conversion of the SC is too small.

Several aspects contributing to the total error in the determination of tropospheric NO₂ columns from the satellite measurements were studied by Boersma et al. (2004). In that analysis was concluded that including realistic aerosol in the radiative transfer calculations would increase the airmass factors by up to 40% depending on aerosol type and aerosol optical depth. The vertical profile of the aerosols was assumed to be exponential with a scale height of 2.0 km and the vertical NO₂ profile was not specified. The conclusion from this study was that the correction for the aerosol impact cannot be simply separated from the effect of clouds and that if a cloud retrieval scheme is adopted, it will account for a large part of the aerosol effect by retrieving a different cloud fraction and height. Martin et al. (2003) also analysed the aerosol impact on the airmass factor applied in the retrieval process. Monthly aerosol properties derived with the GOCART model were used for that study. The authors found that biomass burning aerosol and desert dust would reduce the AMF by 10–20% while over industrial regions an increase of 5–10% was observed.

**Aerosol impact on
the NO₂ airmass
factor**

J. I. Leitão et al.

[Title Page](#)[Abstract](#)[Introduction](#)[Conclusions](#)[References](#)[Tables](#)[Figures](#)[⏪](#)[⏩](#)[◀](#)[▶](#)[Back](#)[Close](#)[Full Screen / Esc](#)[Printer-friendly Version](#)[Interactive Discussion](#)

**Aerosol impact on
the NO₂ airmass
factor**

J. Leitão et al.

[Title Page](#)[Abstract](#)[Introduction](#)[Conclusions](#)[References](#)[Tables](#)[Figures](#)[⏪](#)[⏩](#)[◀](#)[▶](#)[Back](#)[Close](#)[Full Screen / Esc](#)[Printer-friendly Version](#)[Interactive Discussion](#)

A similar sensitivity study to the one presented here was carried out by Gloudemans et al. (2008) to analyse, among other aspects, the impact of aerosols in the retrieval of CH₄ and CO (in the IR region) from the SCIAMACHY instrument. One of the main findings from this study was that, depending on the location of the plume and type of aerosol, the omission of aerosol influence in the retrieval process can lead to significant errors in the total column of CH₄. Thomas et al. (2005), with a similar study for SO₂ (retrieved in the UV region) concluded that aerosols are relevant mainly for optical thickness above 0.3 and in the presence of desert dust plumes in the boundary layer (BL). If these two conditions were realised at the same time the authors estimated that the column would be underestimated by 5–10%. For the TOMS SO₂ retrieval, Krueger et al. (1995) showed that neglecting a rather thin aerosol layer may result in a systematic overestimation of the retrieved total SO₂ content.

Furthermore, recently, the aerosol impact on ground-based zenith-sky DOAS measurements was also investigated by Chen et al. (2009). The aerosol effect was studied by changing the extension of aerosol and NO₂ layers, together and independently of each other, and varying also the SSA. From this analysis an error of 10% was determined. Nevertheless, for these measurements, the uncertainties caused by unknown aerosol properties and vertical profiles of both aerosol and NO₂ tended to cancel each other.

In current retrieval methods the presence of aerosols in the atmosphere is included in many different ways. Some retrieval processes do not explicitly correct for aerosol impact, arguing that the cloud correction scheme also accounts for a large part of the aerosol effect (Boersma et al., 2004, 2007). Another approach is to use a static a priori profile for aerosol loading and type (Nüß, 2005; Richter et al., 2005). Finally, some retrievals include full aerosol treatment in the radiative transfer using aerosol fields from models (Martin et al., 2003; Lee et al., 2009). However, none of these options will actually be able to accurately identify the type of aerosols (with its properties) and its distribution at the time and location of measurements.

2 Methodology

Numerous factors need to be accounted for when considering the effect of aerosols on the NO₂ measurements. In the present study, these effects were analysed in detail by considering multiple scenarios where the aerosol vertical distribution was varied together with its load and optical properties. In addition, the NO₂ vertical profile was also varied. In a first step, simplified scenarios were investigated with, for example, NO₂ and aerosol vertical distribution as box profiles and considering purely scattering or partly absorbing aerosols. The results from these simulations provide insight into the direction and magnitude of the effects of different parameters on the satellite sensitivity. More realistic results were obtained in a second phase where measured aerosol profiles from different locations were used and the NO₂ profiles considered were taken from model simulations for urban and rural conditions. In both cases, the interference exerted by aerosols can then be analysed by comparing these scenarios with a reference scenario where no aerosol is considered in the radiative transfer calculations.

2.1 General radiative transfer settings

Airmass factors were calculated with the radiative transfer model SCIATRAN 2.2 (Rozanov et al., 2005). The calculations were performed at four different wavelengths (425, 437.5, 440 and 450 nm), in nadir observation, and six solar zenith angles (SZA, from 20° to 70° in steps of 10°). SCIATRAN was operated using the discrete ordinate method for solution of the radiative transfer equation in plane parallel geometry accounting for full multiple scattering effects. At the viewing geometry used here, the effects of Earth's curvature and refraction can be neglected. The surface albedo was set to 0.03 assuming that this is, for the spectral range used, an average value for urban areas.

Aerosol impact on the NO₂ airmass factor

J. Leitão et al.

Title Page

Abstract

Introduction

Conclusions

References

Tables

Figures

◀

▶

◀

▶

Back

Close

Full Screen / Esc

Printer-friendly Version

Interactive Discussion



2.2 NO₂ profile

For the initial analysis, the NO₂ profiles were defined as simplified box profiles, where the NO₂ is homogeneously distributed within a boundary layer of either 600 m or 1.0 km or 2.0 km height. This homogeneous distribution is, most probably, not often found close to the major anthropogenic sources, i.e. in urban locations. For that reason, in the final case scenarios simulated, two different NO₂ profiles, from surface to 6.5 km, were used: average urban and rural. These profiles are an average from CHIMERE (Schmidt et al., 2001; Honoré et al., 2008) model runs with a 9×9 km² resolution and for the period from 23 May to 11 June 2007 (randomly selected). The NO₂ volume mixing ratio above 6.5 km decreases slowly to a value of 1.5×10^{-6} ppm at 100 km. The model results are based on a simulation for Paris downtown, a location in the close vicinity of Paris at 15 km East and a rural region at 100 km East of Paris. Since the first two sites are very similar, and, considering that the typical size of a satellite pixel would include both of these measurements, their average is defined as average urban – “Avg Urb”. In Fig. 2 the different NO₂ mixing ratio profiles are shown from surface up to 10 km.

As it can be seen in the profiles presented in Fig. 2, the NO₂ profile determined by the model for the urban conditions is not at all similar to a homogeneous distribution over a boundary layer of 1.0 km or even 600 m. This has a significant impact on the results as it will be further discussed in Sect. 3.2. In addition, the large difference between the urban and rural profiles illustrates how the NO₂ vertical distribution can show significant variations over a short distance. This might be a crucial point for satellite retrievals where, at the spatial resolution of current a priori data, both urban and rural scenes are often contained in one model grid cell (Heckel et al., 2009).

2.3 Aerosol settings

Currently, several datasets with aerosol characteristics are available from records of either ground-based or satellite instruments. Worldwide ground-based networks offer the possibility to obtain crucial information to better characterize aerosols and reduce

Aerosol impact on the NO₂ air mass factor

J. Leitão et al.

Title Page

Abstract

Introduction

Conclusions

References

Tables

Figures

⏪

⏩

◀

▶

Back

Close

Full Screen / Esc

Printer-friendly Version

Interactive Discussion



the current uncertainties on the definition of aerosol optical properties. This is the case of, for instance, the Aerosol Robotic Network (AERONET, Holben et al., 1998) that provides long-term and continuous measurements of aerosol optical, microphysical and radiative properties (e.g. AOD). In addition, data is also provided from many lidar networks established in different continents, such as the European Aerosol Research Lidar Network (EARLINET, Mattis et al., 2002), or the Asian dust network (AD-net, Murayama et al., 2001) that monitor both the horizontal and vertical distribution of aerosols and its optical properties. In the present study data taken from these networks was applied in the definition of the aerosol optical properties and its vertical distribution. However, these data are not the only source of information as, nowadays, many of the instruments flying on different satellites measure the same features with the advantage of broad spatial coverage (e.g. MODIS, MISR, MERIS, CALIPSO, etc.).

The aerosol settings used in the radiative transfer model are linked to the optical properties and vertical profiles. These are based on data from measurements so that they can be a better representation of the atmospheric aerosol characteristics. The optical properties and size distributions of aerosol, at 440 nm, were mainly taken from records of 12 worldwide AERONET stations presented in Dubovik et al. (2002). This dataset is representative for the usual classification of four different aerosol types that have distinctive physicochemical, optical and radiative properties: urban/industrial, biomass burning, desert dust and oceanic. The precision of the AERONET dataset is discussed in detail in several publications but this subject will not be explored here because the accuracy of these measurements and representativeness of the dataset is not central to the conclusions to be drawn.

Aerosols emitted in urban areas and from open vegetation fires are, on average, dominated by small particles (Seinfeld and Pandis, 1998). Yet, the size distribution of this aerosol, especially that of biomass burning cases, is not constant and varies in time and space. The dimension of the particles is mostly dependent on the type of fuel, the combustion phase and the age of smoke (e.g. Dubovik et al., 2002). This last factor can be important when considering fire plumes that are transported for some days away

**Aerosol impact on
the NO₂ airmass
factor**

J. Leitão et al.

[Title Page](#)[Abstract](#)[Introduction](#)[Conclusions](#)[References](#)[Tables](#)[Figures](#)[⏪](#)[⏩](#)[◀](#)[▶](#)[Back](#)[Close](#)[Full Screen / Esc](#)[Printer-friendly Version](#)[Interactive Discussion](#)

**Aerosol impact on
the NO₂ airmass
factor**

J. Leitão et al.

Title Page

Abstract

Introduction

Conclusions

References

Tables

Figures

◀

▶

◀

▶

Back

Close

Full Screen / Esc

Printer-friendly Version

Interactive Discussion

from the source. On the other hand, mostly coarse particles are found in desert dust scenes or oceanic aerosol (Seinfeld and Pandis, 1998). The selection of results presented here will follow these assumptions, i.e. not every simulated case will be shown but mostly those which are more representative of the aerosol type in consideration. In order to facilitate the interpretation of results, a mixing of fine and coarse aerosol, as it would happen in reality, was not simulated. For each of the aerosol types, the phase functions (see Fig. 3) for both fine and coarse particles were considered. These angular distributions of scattered light were determined with a FORTRAN program developed by Michael Mishchenko available at <http://www.giss.nasa.gov/staff/mmishchenko/brf/>.

In the first phase of the study, the aerosol vertical distribution was defined as a box shaped profile with variable height and with extinction coefficients representative for three aerosol loads: 0.1 (low pollution level), 0.5 (moderate pollution) and 0.9 (heavily polluted scene) aerosol optical depth. Aerosol absorption was set to the average from all the SSA (ω_0) values given at 440 nm in Dubovik et al. (2002): 0.93. The SSA differs according to type and source of aerosol and, therefore, is in part dependent on the location of measurement (see, for example, Hu et al., 2007). Thus, this parameter was varied between 0.8 and 0.95 and the changes in the AMF analyzed as well (see Sect. 3.4). For the majority of the scenarios, the impact of aerosol absorption was simply investigated by comparing the AMF determined with runs where ω_0 was set to 0.93 and others where $\omega_0=1.0$. This allowed determining the maximum effect in the results when reducing the absorbing ability of aerosol.

As mentioned above, the first set of scenarios considers well defined layers of homogeneously distributed aerosol. Alternatively, the aerosol's vertical distribution was defined in different ways: following the NO₂ profile; starting at surface level and with the top layer lower or higher than that of the NO₂ profile; furthermore, discrete elevated aerosol layers above the NO₂ layer (in the BL) were also taken into account. The different combinations of NO₂ and aerosol box layers are summarized in Table 1.

The scenarios A to H will probably not be realised for all types of aerosols. Normally, the urban aerosol is assumed to be either in homogenous layers extending from the surface to the top of BL or, often, following an exponential decrease with height. In general, one can assume that the majority of anthropogenic sources are the same for both NO₂ and aerosols and, therefore, they would have similar spatial distributions. However, depending on the source location and transport processes, the aerosol layer can extend to a higher altitude, whereas NO₂ will be in general more concentrated closer to the source region and at lower levels, due to a shorter life time. For that reason, the extension of each layer was also varied independently so that different scenarios could be analysed. The scenarios with elevated discrete aerosol layers are mostly adequate to illustrate plumes of biomass burning smoke and desert dust that are transported several hundreds to thousand kilometres away from the source and which can be lifted to higher altitudes during transport. Several studies have registered aerosol from fire events transported to great distances away from the initial source region: smoke from fires in the African savanna that is transported across the Atlantic Ocean (Husar et al., 1997; Ansmann et al., 2009); emissions from boreal fires in Siberia and/or Canada (Damoah et al., 2004; Murayama et al., 2004; Müller et al., 2005); or, on a more regional scale, the transport within Europe (Amiridis et al., 2009). This long range transport often occurs in the free troposphere, but the plumes will also be part of the boundary layer either by intrusion processes or due to the low initial injection height (Müller et al., 2003; Labonne et al., 2007). These same processes also take place with desert dust plumes (Husar et al., 1997) and in some occasions the desert particles are found from the low troposphere to much higher above in the atmosphere (Mattis et al., 2002; Murayama et al., 2003). Desert storms are responsible for a great fraction of aerosol emissions and most of it is released either from the Sahara or the Asian deserts, in particular Gobi and Taklimakan. Dust outbreaks from these deserts often can mix with urban type aerosol emitted within European or Asian cities (e.g. Zhou et al., 2002; Papayannis et al., 2008).

**Aerosol impact on
the NO₂ airmass
factor**

J. Leitão et al.

Title Page

Abstract

Introduction

Conclusions

References

Tables

Figures

◀

▶

◀

▶

Back

Close

Full Screen / Esc

Printer-friendly Version

Interactive Discussion



**Aerosol impact on
the NO₂ airmass
factor**

J. Leitão et al.

Title Page

Abstract

Introduction

Conclusions

References

Tables

Figures

◀

▶

◀

▶

Back

Close

Full Screen / Esc

Printer-friendly Version

Interactive Discussion



In the attempt of simulating more realistic situations than those described above, in a second stage, the definition of the case studies was based on data available from different measurement datasets. The size distribution and corresponding phase functions were maintained from the initial stage. Nevertheless, the extinction coefficients used for the profile definition were based on lidar measurements performed at numerous locations at different times of the year (see representation of profiles in Fig. 4). Still, the profiles considered in this study are not the exact representation of the original ones. Often adjustments were required in order to obtain a profile from surface to the top of atmosphere of 100 km. Moreover, as these are meant to be examples for case studies their representativeness is not a subject of this analysis and do not influence the conclusions drawn.

The ω_0 values required to determine absorption coefficients were either taken from the corresponding records or based on typical values available from other studies that focused specifically on each of the aerosol types. Because lidar measurements (both satellite and ground-based) are usually performed at 355 nm and/or 532 nm an Ångström exponent (Ångström, 1929) was necessary to convert these values to the corresponding ones at 440 nm (within the wavelength region where NO₂ is retrieved). These values were also taken from the referred literature. A compilation of the settings used for the scenarios of the final phase of this study is presented in Table 2. The oceanic aerosol type was not included at this stage because this aerosol is normally only observed in very low concentrations at polluted sites and is usually mixed with other types of aerosol. Therefore, for simplicity of the analysis, it is assumed that its influence in the NO₂ retrieval is similar to that of the other types considered.

3 Results

A comprehensive analysis was performed with airmass factors of NO₂ calculated for many different case studies. The results presented in this section are structured in change of input parameter in the radiative transfer calculations. First the boundary

layer variations are analysed, followed by impact in modifications of the extension of aerosol layer and ending in the single scattering albedo effects. For completeness of the study, the NO₂ AMFs were calculated with all different types of aerosol with all profiles considered. However, depending on the aerosol source, the typical size and vertical distribution are quite different. For that reason, the results presented in the next sections are focused on the more realistic cases, considering also the results from the second phase of the analysis when measured aerosol profiles were used. In addition, all results presented here were calculated at 440 nm as this is the wavelength for which the AERONET aerosol optical properties are given. Extension of the calculations to the wavelength range often used for NO₂ retrieval revealed an average increase of AMF by 10% from 425 to 450 nm. This variation is relatively small and will largely cancel if it is linear with wavelength but might be relevant in some cases. For different solar zenith angles (SZA), the general trend shows that the AMF increases for higher sun, but for specific cases, this tendency can also be reverted. In some circumstances (not presented here), when considering fine aerosol, a decrease occurs with high sun, and in other cases, with coarse particles, a small increase is then followed by decay after 50° or 60°. The variation of the size parameters (mean radius and its standard deviation within the fine or coarse mode categories) of the different aerosol types representative for the locations considered in this study was rather small. The similarity in values resulted in nearly identical phase functions with noticeable differences only between the two general size distributions considered: fine and coarse (see Fig. 3). As a result, the NO₂ AMF determined within the various scenarios with fine particles are very similar, and the same occurs for those with coarse aerosol. When comparing to the scenario without aerosol it was found that fine particles have a higher impact on intensifying the changes on the AMF than the coarse ones. However, this effect depends on many factors such as the vertical distribution or sun position (e.g. very low sun can favour the enhancement of signal by the coarse particles standing in a discrete layer above the trace gas). As expected the values of AMF determined with non-absorbing aerosol were the highest. This decrease in the measurements' sensitivity for absorbing aerosol

**Aerosol impact on
the NO₂ airmass
factor**

J. Leitão et al.

[Title Page](#)[Abstract](#)[Introduction](#)[Conclusions](#)[References](#)[Tables](#)[Figures](#)[⏪](#)[⏩](#)[◀](#)[▶](#)[Back](#)[Close](#)[Full Screen / Esc](#)[Printer-friendly Version](#)[Interactive Discussion](#)

is a consequence of the reduction of available light when such aerosol is present in the atmosphere. It is also important to note that at 440 nm the Rayleigh optical thickness is 0.32. Consequently, in scenarios I and N, the molecular scattering dominates.

3.1 Changes in boundary layer height

5 The height of the boundary layer differs for different locations and is also dependent on seasonal variations. To investigate the effect of BL height changes alone, a study was carried out varying this height to 0.6, 1.0 and 2.0 km, and maintaining both the NO₂ and aerosol homogeneously distributed in this layer. In Fig. 5 the results obtained for urban fine and coarse aerosol with different aerosol optical thickness are presented.

10 These results show that an increase of the BL height leads to an increase of AMF values. Consequently, if a too low the BL height is assumed in the retrieval, the tropospheric columns of NO₂ will be overestimated. The AMF increases by about 20% when the boundary layer top changes from 0.6 to 2.0 km. The largest effect was found for the simulation with coarse aerosol and optical thickness of 0.1 with 37% variation, at 440 nm. Interestingly, the effect seems to decrease with growing aerosol load. Such a variation is probably a result of the increase in scattering (and therefore the effective albedo) which will improve the sensitivity of the satellite measurements to the lower atmosphere. For every case it was found that the smallest AMFs are determined for the conditions without aerosol (not shown). Thus, one can conclude that, in these scenarios, the presence of aerosol contributes to an increase of the sensitivity of the measurements, even if quite small for coarse particles and low aerosol load. In practice, this indicates that, for the cases exemplified here, if aerosol is not accounted for in the retrieval, the NO₂ VC will be overestimated.

25 The figure also reveals, as mentioned above, the difference in behaviour between fine and coarse particles. The AMFs resulting from the simulations with fine aerosol mixed with the trace gas are higher, i.e. at the same AOD, fine aerosol increases the sensitivity to the NO₂ more than coarse particles, and this difference of results increases with AOD. This is probably related to the less pronounced forward peak in

Aerosol impact on the NO₂ airmass factor

J. Leitão et al.

Title Page

Abstract

Introduction

Conclusions

References

Tables

Figures



Back

Close

Full Screen / Esc

Printer-friendly Version

Interactive Discussion



scattering on fine particles (see phase function in Fig. 3) which increases the ratio of photons scattered towards the satellite under this observation geometry and therefore improves the sensitivity.

3.2 Changes in extension of aerosol layer

5 In the previous section, NO₂ and aerosol had the same vertical profiles representing a situation where both are well mixed. In the following scenarios, the vertical extension of the aerosol layer was varied while the NO₂ profile was kept constant. This was done for two NO₂ profiles, a simple 1.0 km box profile and the more realistic urban profile as modelled by CHIMERE. Figure 6 shows the results side by side for different AODs.

10 As it can be observed, in general, any aerosol mixed with the trace gas tends to enhance the NO₂ signal, indicating that an overestimation of the NO₂ VC will likely occur when the aerosol presence is neglected in the retrieval. However, the magnitude of the influence does vary as it depends on the relative position of trace gas and aerosol, in particular the aerosol load above the trace gas. In addition, the size of the particles also plays a role in the calculations. As for the box profiles discussed above, at the same AOD, fine particles have a larger influence on the airmass factors, due to the
15 generally higher backscattering (see Fig. 3).

In the simulations with box profiles, the interplay between reduction and enhancement of sensitivity can explain the observed variations: if the aerosol layer is close to the surface, i.e. with its top at 600 m, below the top of the trace gas layer, the sensitivity will be enhanced due to higher reflectivity and multiple scattering. An increase of the AMF by 11% on average is found when the top of aerosol layer lowers from 1.0 km to the 600 m and, in the case of highly polluted scenes with AOD=0.9, the difference between the values can be as high as 25%. Compared to the simulation without aerosol,
20 the sensitivity can be enhanced by up to a factor of two. On the other hand, when the aerosol layer extends higher than the layer of NO₂, the AMF is lower (by 5 to 45%) than in the case when both aerosol and NO₂ have the top layer at 1.0 km. This results from the elevated part of the layer of aerosol that acts as a shield and thereby partly

Aerosol impact on the NO₂ airmass factor

J. Leitão et al.

Title Page

Abstract

Introduction

Conclusions

References

Tables

Figures

◀

▶

◀

▶

Back

Close

Full Screen / Esc

Printer-friendly Version

Interactive Discussion



cancels the enhancement of sensitivity in the lower part. Still, compared to the AMF values obtained without aerosol, the fine particles will slightly increase the NO_2 signal, with the exception of high solar zenith angles. In comparison, the coarse particles have smaller influence on the measurements.

5 The differences found in the AMFs calculated with $\text{AOD}=0.1$ and higher values indicate the importance of using the right AOD in the retrieval. An underestimation of the AOD will lead to an overestimation of the VC. The scenario F (aerosol layer extending to 2.0 km) is an exception to this statement as the AMF values do not vary much for different AODs.

10 In qualitative terms, the interpretation of the scenarios with the urban NO_2 profile is quite similar. However, for the latter, the AMF values are smaller as the NO_2 is more concentrated at the surface where the satellite sensitivity is the smallest. This is directly observed in the “no aerosol” case where the AMF decreases from 0.81 (at 440 nm and 40° SZA) to 0.70 (due to the shielding effect related to Rayleigh scattering). In addition, shielding effect of aerosols is also more pronounced for the NO_2 urban profile than for the 1.0 km box one, leading to an overall reduced effect of aerosols. In the case with an aerosol layer of coarse particles above the NO_2 , even a slight decrease in the AMF is observed. Thus overall the importance of aerosols is reduced if a more realistic NO_2 profile is assumed.

20 The model profiles were also combined with aerosol profiles derived from measurements in background areas (scenario I) and urban environments (scenarios J and K). The results are shown in Fig. 7 for calculations assuming fine and coarse particles separately. Clearly, in these particular circumstances, the aerosol effect is much smaller than before, and very close to zero in the case of typical background profiles for both the NO_2 and aerosol. Independently of its detailed shape, the presence of an aerosol layer tends to cover the NO_2 layer below thereby decreasing the sensitivity of the measurements to trace gas amounts close to the surface. Depending on the sun position and the aerosol profile, small enhancements as well as reductions in sensitivity can occur. This emphasises the point that the sensitivity of the measurements does not only

Aerosol impact on the NO_2 airmass factor

J. Leitão et al.

Title Page

Abstract

Introduction

Conclusions

References

Tables

Figures

◀

▶

◀

▶

Back

Close

Full Screen / Esc

Printer-friendly Version

Interactive Discussion



depend on the vertical distribution or total load of the aerosol but the combined effect of both, aerosol and NO_2 distribution. For coarse particles all the AMFs were smaller than for the case without aerosol, indicating that the aerosol might be preventing light from reaching down lower into the NO_2 layer close to the surface (or back from this layer to the satellite instrument).

3.3 Changes in the position of the aerosol layer

The transport of dust plumes into European and certain Asian cities is not a rare event. Similarly, aerosol emitted from biomass burning events can undergo long-range transport and reach regions with anthropogenic pollution. These plumes are not only observed in the free troposphere but can, sporadically, make a large contribution to the aerosol load measured in the boundary layer. Scenarios D, E and G (see Table 1) are simplified representations of such events with aerosol mostly being concentrated at higher altitudes. The results from these runs lead to the same conclusions as before, i.e. an aerosol layer standing above the trace gas obstructs the observation from space (see Fig. 8). A decrease of 6% to ~70% is observed when comparing the AMFs obtained for the scenario without aerosol and that with aerosol distributed from 1.0 to 2.0 km. This reduction is higher for larger aerosol load, i.e. optical thickness of 0.9. If such plumes, standing in high altitudes, are not accounted for in the retrieval process, the tropospheric VCs are underestimated. The differences of the results for the layers 1.0 to 2.0 km and 2.0 to 3.0 km (not presented here) were not significant. This indicates that the height of the aerosol layer is not so relevant for the sensitivity of the measurements when there is no overlap of the layers of trace gas and aerosol. Contrary to this, in the case of aerosol mixed with NO_2 in the top of the layer (from 0.6 to 1.0 km) it was possible to notice (Fig. 8) that the particles do not interfere much with the measurements of the trace gas (cancelling of albedo and shielding effect). In fact, only with small particles present will a slight enhancement (~10% maximum) of the columns be registered. It should be noted though, that the effect of aerosol on NO_2 present within

Aerosol impact on the NO_2 air mass factor

J. Leitão et al.

Title Page

Abstract

Introduction

Conclusions

References

Tables

Figures

◀

▶

◀

▶

Back

Close

Full Screen / Esc

Printer-friendly Version

Interactive Discussion



a biomass burning plume will be quite different than that on NO_2 in the boundary layer as discussed here.

In a more realistic scenario, aerosols are also present close to surface in urban areas. Therefore, profiles have been defined to include both the local plumes and those of long-range transport from biomass burning smoke or desert dust (e.g. scenarios L and P from Table 2). An example of these results is presented in Fig. 9 for desert dust layers and fire plumes measured over different cities across the globe. As it can be seen from these findings, the effect of the aerosol layers transported above polluted areas can be quite different. Once more, the reduction in the sensitivity of the measurements, when compared with the “no aerosol” case, can be negligible or as large as $\sim 110\%$ (for scenario O). This pronounced reduction is caused by the combination of several factors: the large optical depth of the aerosol ($\text{AOD}=1.05$); its absorbing nature ($\omega_0=0.92$); and the small fraction of particles that are mixed with the trace gas. This distribution of aerosol is the main difference between scenario L and O. The aerosol close to the surface present in scenario L may contribute to the cancelling of the shielding effect and therefore explain the large discrepancy between the results of the scenarios. In the case of simulations M, N and P the AMFs are not so reduced mainly because of the lower aerosol loads.

For the desert dust cases, only coarse aerosol was considered in the radiative transfer calculations but both fine and coarse (not presented here) particles were used for the biomass burning situations. The difference in the AMF calculated with each of the aerosol types is in the order of 20–25% with the higher values obtained for the runs with fine aerosol.

3.4 Changes in single scattering albedo

As mentioned above, for all the scenarios including box profiles the AMF were calculated both for a single scattering albedo (SSA) of 0.93 and 1 (not presented here). However, the SSA varies in time and space. Thus, the effect of deviations in the SSA in the radiative transfer calculations was also tested by changing this parameter to 0.80

Aerosol impact on the NO_2 air mass factor

J. Leitão et al.

Title Page

Abstract

Introduction

Conclusions

References

Tables

Figures

⏪

⏩

◀

▶

Back

Close

Full Screen / Esc

Printer-friendly Version

Interactive Discussion



and 0.95. These results are presented for both the simulations performed with the box profiles in scenario C (Fig. 10) and scenarios J and O (Fig. 11) where the NO₂ modelled profiles and measured aerosol vertical distribution were considered (see Table 1 and Table 2 for more details on scenarios definitions). As expected, the SSA can have a great impact on the calculation of the AMF. An increase in the absorbing properties of the aerosol (SSA decreases from 0.95 to 0.8) results in a general decrease of the AMF. While for low aerosol load the increase is in the order of 5–10%, in the highly polluted atmosphere with AOD=1.05 the effect of SSA on the AMF can be as high as 84%. Still, the variation of the AMF values is not only dependent on the aerosol amount but also on the profiles considered. The variation of the AMF caused by the changes in the SSA values was found to vary for different aerosol vertical distributions.

4 Conclusions

Aerosols can have a significant impact on the retrieval of tropospheric trace gases using UV/visible nadir measurements from space. In order to identify and quantify this impact, the effects of different aerosol parameters were investigated using both idealised and realistic scenarios. Overall, a large variability in the results was observed with examples of both, increases and decreases of sensitivity. The most important factors for the satellite sensitivity are the relative vertical distribution of aerosol and NO₂, the AOD and the SSA. On the other hand, it was concluded that detailed differentiation of the size distribution of the aerosol is not a priority for the retrieval process. Differences in the air mass factors were found when applying either coarse or fine aerosol. However, no large differences were evident when considering diverse size distributions within the two main types.

Variations of the vertical extension of a well mixed boundary layer of 1.0 km can result in large differences (max. 26%) of the air mass factors calculated, especially when the aerosol load is low and in low sun conditions. The boundary layer height has strong seasonal, daily, and diurnal variations and not accounting for these changes will

Aerosol impact on the NO₂ air mass factor

J. Leitão et al.

Title Page

Abstract

Introduction

Conclusions

References

Tables

Figures

◀

▶

◀

▶

Back

Close

Full Screen / Esc

Printer-friendly Version

Interactive Discussion



contribute to the inaccuracy of the calculated columns. The determined AMFs indicate that, if the boundary layer height is underestimated in the a priori, the tropospheric NO₂ column will be overestimated (and vice-versa).

Aerosol mixed with the trace gas, even if only partly, will, by means of increased effective albedo and multiple scattering, enhance the NO₂ signal. In contrast, any aerosol layer that stands above the trace gas will act as a shield decreasing the sensitivity of the measurements. If an elevated aerosol layer is not accounted for, the computed NO₂ columns will be too small, and this underestimation can be quite high. The magnitude of these effects will be determined by the relative vertical distribution of aerosol and NO₂. A balance between enhancement and reduction of the signal will occur when the aerosol is both mixed with and above the NO₂ layer. As two examples, the AMF for a 1.0 km layer of NO₂ increases by a factor of two when mixed with a 600 m high aerosol layer of AOD 0.9, while for the case with an aerosol layer of AOD 0.1 between 2.0 to 3.0 km the AMF is reduced by ~78%.

The absorption properties of the particles also play an important role in the retrieval of the trace gas. The largest airmass factors were always obtained for the purely scattering aerosol ($\omega_0=1$). A decreasing SSA reduces the measurement sensitivity. For highly polluted scenes (AOD>0.9) the airmass factor can change by a factor of 1.5 and more when the single scattering albedo is modified from 0.80 to 0.95.

When more realistic vertical profiles were applied for both NO₂ and aerosols, a much smaller effect of aerosol was observed. Large decreases of the sensitivity of the measurements were found only for elevated or largely extended aerosol layers. These situations usually correspond to cases of biomass burning events or desert dust storms. For the urban scenes the changes in the airmass factors were rather small, indicating that in these circumstances, the uncertainties introduced by neglecting the aerosol impact in the retrieval are moderate. Nonetheless, situations of highly polluted scenes, as those of megacities, were not exactly represented here (AOD can be much higher than 0.9). Thus, in order to allow a better understanding of the aerosol influence in the measured NO₂ columns, in these circumstances, further analysis is still required.

Aerosol impact on the NO₂ airmass factor

J. Leitão et al.

Title Page

Abstract

Introduction

Conclusions

References

Tables

Figures

◀

▶

◀

▶

Back

Close

Full Screen / Esc

Printer-friendly Version

Interactive Discussion



In the present study, only clear sky cases have been considered. For partially cloudy scenes the results would differ in particular if the data are corrected for cloud effects. The presence of aerosols will also impact on the retrieved cloud properties as discussed in Boersma et al. (2004). Bearing in mind that for many scenarios evaluated here the effect of aerosols is to enhance the measurement sensitivity, it is not clear if the resulting increase in cloud fraction and cloud top pressure would actually compensate the effect of aerosols or rather enhance it.

The continuing use of fossil fuels and biomass burning in a changing climate will result in changes in the amounts and distribution of NO_x which is one of the key precursors for tropospheric ozone. To assess accurately these changes and the efficiently allocate efforts to mitigate pollution, precise knowledge of the global tropospheric column of NO_2 is essential. This study shows that to improve our current knowledge of the global distributions of tropospheric NO_2 , and its evolution, improved knowledge of the aerosol properties are required. These include the vertical profile, AOD, size distribution and also the scattering/absorption properties of the particles. Such data would preferably come from simultaneous measurements of trace gas and aerosol properties from space or alternatively from a combination of satellite and ground-based measurements with model predictions.

Acknowledgements. This study was in part supported by the GEMS project funded by the European Commission as part of its Sixth Framework Programme and by the University of Bremen. We acknowledge the AERONET and EARLINET networks for the provision of aerosol datasets used in this study. In addition, we would like to thank Chieko Kittaka and David Winker who kindly provided CALIPSO climatologies. Finally, we would like to thank V. Rozanov, A. Rozanov and further SCIATRAN developers for the provision of the model and support throughout the study.

**Aerosol impact on
the NO_2 airmass
factor**

J. Leitão et al.

Title Page

Abstract

Introduction

Conclusions

References

Tables

Figures

◀

▶

◀

▶

Back

Close

Full Screen / Esc

Printer-friendly Version

Interactive Discussion



References

- Akimoto, H.: Global air quality and pollution, *Science*, 302, 1716–1719, 2003.
- Amiridis, V., Balis, D. S., Giannakaki, E., Stohl, A., Kazadzis, S., Koukouli, M. E., and Zanis, P.: Optical characteristics of biomass burning aerosols over Southeastern Europe determined from UV-Raman lidar measurements, *Atmos. Chem. Phys.*, 9, 2431–2440, 2009, <http://www.atmos-chem-phys.net/9/2431/2009/>.
- Ångström, A.: On the atmospheric transmission of Sun radiation and on dust in the air, *Geogr. Ann.*, 11, 156–166, 1929.
- Ansmann, A., Baars, H., Tesche, M., Müller, D., Althausen, D., Engelmann, R., Pauliquevis, T., and Artaxo, P.: Dust and smoke transport from Africa to South America: Lidar profiling over Cape Verde and the Amazon rainforest, *Geophys. Res. Lett.*, 36, L11802, doi:10.1029/2009GL037923, 2009.
- Balis, D. S., Amiridis, V., Zerefos, C., Gerasopoulos, E., Andreae, M., Zanis, P., Kazantzidis, A., Kazadzis, S., and Papayannis, A.: Raman lidar and sunphotometric measurements of aerosol optical properties over Thessaloniki, Greece during a biomass burning episode, *Atmos. Environ.*, 37, 4529–4538, 2003.
- Beirle, S., Platt, U., von Glasow, R., Wenig, M., and Wagner, T.: Estimate of nitrogen oxide emissions from shipping by satellite remote sensing, *Geophys. Res. Lett.*, 31, L18102, doi:10.1029/2004GL020312, 2004.
- Beirle, S., Salzmann, M., Lawrence, M. G., and Wagner, T.: Sensitivity of satellite observations for freshly produced lightning NO_x, *Atmos. Chem. Phys.*, 9, 1077–1094, 2009, <http://www.atmos-chem-phys.net/9/1077/2009/>.
- Bézy, J.-L., Delwart, S., and Rast, M.: MERIS – a new generation of ocean colour sensor onboard ENVISAT, *ESA Bull.*, 103, 48–56, 2000.
- Boersma, K. F., Eskes, H. J., and Brinksma, E. J.: Error analysis for tropospheric NO₂ retrieval from space, *J. Geophys. Res.*, 109, D04311, doi:10.1029/2003JD003962, 2004.
- Boersma, K. F., Eskes, H. J., Veefkind, J. P., Brinksma, E. J., van der A, R. J., Sneep, M., van den Oord, G. H. J., Levelt, P. F., Stammes, P., Gleason, J. F., and Bucsela, E. J.: Near-real time retrieval of tropospheric NO₂ from OMI, *Atmos. Chem. Phys.*, 7, 2103–2118, 2007, <http://www.atmos-chem-phys.net/7/2103/2007/>.

AMTD

2, 3221–3264, 2009

Aerosol impact on the NO₂ airmass factor

J. Leitão et al.

Title Page

Abstract

Introduction

Conclusions

References

Tables

Figures

◀

▶

◀

▶

Back

Close

Full Screen / Esc

Printer-friendly Version

Interactive Discussion



**Aerosol impact on
the NO₂ air mass
factor**

J. Leitão et al.

- Bovensmann, H., Burrows, J. P., Buchwitz, M., Frerick, J., Noel, S., Rozanov, V. V., Chance, K. V., and Goede, A. P. H.: SCIAMACHY: Mission objectives and measurement modes, *J. Atmos. Sci.*, 56(2), 127–150, doi:10.1175/1520-0469, 1999.
- Burrows, J. P., Holzle, E., Goede, A. P. H., Visser, H., and Fricke, W.: SCIAMACHY – Scanning Imaging Absorption Spectrometer for Atmospheric Chartography, *Acta Astronaut.*, 35, 445–451, 1995.
- Burrows, J. P., Weber, M., Buchwitz, M., Rozanov, V., Ladstätter-Weißenmayer, A., Richter, A., DeBeek, R., Hoogen, R., Bramstedt, K., Eichmann, K.-U., Eisinger, M., and Perner, D.: The Global Ozone Monitoring Experiment (GOME): Mission concept and first scientific results, *J. Atmos. Sci.*, 56(2), 151–175, doi:10.1175/1520-0469, 1999.
- Callies, J., Corpaccioli, E., Eisinger, M., Hahne, A., and Lefebvre, A.: GOME-2 – Metop’s second generation sensor for operational ozone monitoring, *ESA Bull.*, 102, 28–36, 2000.
- Chang, D., Song, Y., and Liu, B.: Visibility trends in six megacities in China 1973–2007, *Atmos. Res.*, 94, 161–167, 2009.
- Chazette, P., Randriamiarisoa, H., Sanak, J., Couvert, P., and Flamant, C.: Optical properties of urban aerosol from airborne and ground-based in situ measurements performed during the Etude et Simulation de la Qualité de l’air en Ile de France (ESQUIF) program, *J. Geophys. Res.*, 110, D02206, doi:10.1029/2004JD004810, 2005.
- Chen, D., Zhou, B., Beirle, S., Chen, L. M., and Wagner, T.: Tropospheric NO₂ column densities deduced from zenith-sky DOAS measurements in Shanghai, China, and their application to satellite validation, *Atmos. Chem. Phys.*, 9, 3641–3662, 2009, <http://www.atmos-chem-phys.net/9/3641/2009/>.
- Damoah, R., Spichtinger, N., Forster, C., James, P., Mattis, I., Wandinger, U., Beirle, S., Wagner, T., and Stohl, A.: Around the world in 17 days – hemispheric-scale transport of forest fire smoke from Russia in May 2003, *Atmos. Chem. Phys.*, 4, 1311–1321, 2004, <http://www.atmos-chem-phys.net/4/1311/2004/>.
- Diner, D. J., Beckert, J. C., Reilly, T. H., Bruegge, C. J., Conel, J. E., Kahn, R. A., Martonchik, J. V., Ackerman, T. P., Davies, R., Gerstel, S. A. W., Gordon, H. R., Muller, J.-P., Myneni, R. B., Sellers, P. J., Pinty, B., and Verstraete, M. M.: Multi-angle Imaging Spectroradiometer (MISR) instrument description and experiment overview, *IEEE Trans. Geosci. Remote*, 36, 1072–1087, 1998.

[Title Page](#)[Abstract](#)[Introduction](#)[Conclusions](#)[References](#)[Tables](#)[Figures](#)[◀](#)[▶](#)[◀](#)[▶](#)[Back](#)[Close](#)[Full Screen / Esc](#)[Printer-friendly Version](#)[Interactive Discussion](#)

Dubovik, O., Holben, B., Eck, T. F., Smirnov, A., Kaufman, Y. F., King, M. D., Tanré, D., and Slutsker, I.: Variability of absorption and optical properties of key aerosol types observed in worldwide locations, *J. Atmos. Sci.*, 59, 590–608, 2002.

5 Gloudemans, A. M. S., Schrijver, H., Hasekamp, O. P., and Aben, I.: Error analysis for CO and CH₄ total column retrievals from SCIAMACHY 2.3 μm spectra, *Atmos. Chem. Phys.*, 8, 3999–4017, 2008,
http://www.atmos-chem-phys.net/8/3999/2008/.

10 Heckel, A., Kim, S.-W., Frost, G. J., Richter, A., Trainer, M., and Burrows, J. P.: Influence of under-sampling in a priori data on tropospheric NO₂ satellite retrievals, *Atmos. Meas. Tech. Discuss.*, to be submitted, 2009.

Hild, L., Richter, A., Rozanov, V., and Burrows, J. P.: Air mass factor calculations for GOME measurements of lightning-produced NO₂, *Adv. Space Res.*, 29(11), 1685–1690, 2002.

15 Holben, B. N., Eck, T. F., Slutsker, I., Tanré, D., Buis, J. P., Setzer, A., Vermote, E., Reagan, J. A., Kaufman, Y., Nakajima, T., Lavenu, F., Jankowiak, I., and Smirnov, A.: AERONET – A federated instrument network and data archive for aerosol characterization, *Remote Sens. Environ.*, 66, 1–16, 1998.

Honoré, C., Rouïl, L., Vautard, R., Beekmann, M., Bessagnet, B., Dufour, A., Elichegaray, C., Flaud, J.-M., Malherbe, L., Meleux, F., Menut, L., Martin, D., Peuch, A., Peuch, V. H., and Poisson, N.: Predictability of European air quality: The assessment of three years of operational forecasts and analyses by the PREV’AIR system, *J. Geophys. Res.*, 113, D04301, doi:10.1029/2007JD008761, 2008.

20 Hu, R.-M., Martin, R. V., and Fairlie, T. D.: Global retrieval of columnar aerosol single scattering albedo from spacebased observations, *J. Geophys. Res.*, 112, D02204, doi:10.1029/2005JD006832, 2007.

25 Husar, R. B., Prospero, J. M., and Stowe, L. L.: Characterization of tropospheric aerosols over the oceans with the NOAA advanced very high resolution radiometer optical thickness operational product, *J. Geophys. Res.*, 102(D14), 16889–16909, 1997.

30 IPCC: Climate Change 2007: The Physical Science Basis. Contribution of Working Group I to the Fourth Assessment Report of the Intergovernmental Panel on Climate Change, edited by: Solomon, S., Qin, D., Manning, M., Chen, Z., Marquis, M., Averyt, K. B., Tignor, M., and Miller, H. L., Cambridge University Press, Cambridge, United Kingdom and New York, NY, USA, 2007.

Aerosol impact on the NO₂ air mass factor

J. Leitão et al.

Title Page

Abstract

Introduction

Conclusions

References

Tables

Figures

◀

▶

◀

▶

Back

Close

Full Screen / Esc

Printer-friendly Version

Interactive Discussion



**Aerosol impact on
the NO₂ air mass
factor**

J. Leitão et al.

[Title Page](#)[Abstract](#)[Introduction](#)[Conclusions](#)[References](#)[Tables](#)[Figures](#)[⏪](#)[⏩](#)[◀](#)[▶](#)[Back](#)[Close](#)[Full Screen / Esc](#)[Printer-friendly Version](#)[Interactive Discussion](#)

King, M. D., Kaufman, Y. J., Menzel, W. P., and Tanré, D.: Remote-sensing of cloud, aerosol, and water-vapor properties from the Moderate Resolution Imaging Spectrometer (MODIS), *IEEE Trans. Geosci. Remote*, 30(1), 2–27, 1992.

Kokhanovsky, A. A. and Rozanov, V. V.: Retrieval of NO₂ vertical columns under cloudy conditions: A sensitivity study based on SCIATRAN calculations, *Atmos. Res.*, 93, 695–699, 2009.

Konovalov, I. B., Beekmann, M., Richter, A., and Burrows, J. P.: Inverse modelling of the spatial distribution of NO_x emissions on a continental scale using satellite data, *Atmos. Chem. Phys.*, 6, 1747–1770, 2006, <http://www.atmos-chem-phys.net/6/1747/2006/>.

Konovalov, I. B., Beekmann, M., Burrows, J. P., and Richter, A.: Satellite measurement based estimates of decadal changes in European nitrogen oxides emissions, *Atmos. Chem. Phys.*, 8, 2623–2641, 2008, <http://www.atmos-chem-phys.net/8/2623/2008/>.

Krueger, A., Walter, L., Bhartia, P. K., Schnetzler, C., Krotkov, N., Sprod, I., and Bluth, G.: Volcanic sulfur dioxide measurements from the total ozone mapping spectrometer instruments, *J. Geophys. Res.*, 100(D7), 14057–14076, 1995.

Labonne, M., Bréon, F.-M., and Chevallier, F.: Injection height of biomass burning aerosols as seen from a spaceborne lidar, *Geophys. Res. Lett.*, 34, L11806, doi:10.1029/2007GL029311, 2007.

Lee, C., Martin, R. V., van Donkelaar, A., O’Byrne, G., Krotkov, N., Richter, A., Huey, G., and Holloways, J. S.: Retrieval of vertical columns of sulfur dioxide from SCIAMACHY and OMI: Air mass factor algorithm development and validation, *J. Geophys. Res.*, 114, D22303, doi:10.1029/2009JD012123, 2009.

Leue, C., Wenig, M., Wagner, T., Klimm, O., Platt, U., and Jähne, B.: Quantitative analysis of emissions from Global Ozone Monitoring Experiment satellite image sequences, *J. Geophys. Res.*, 106(D6), 5493–5505, 2001.

Levelt, P. F., van den Oord, G. H. J., Dobber, M. R., Mälkki, A., Visser, H., de Vries, J., Stammes, P., Lundell, J. O. V., and Saari, H.: The Ozone Monitoring Instrument, *IEEE Trans. Geosci. Remote*, 44(5), 1093–1101, doi:10.1109/TGRS.2006.872333, 2006.

Martin, R. V., Chance, K., Jacob, D. J., Kurosu, T. P., Spurr, R. J. D., Bucsela, E., Gleason, J. F., Palmer, P. I., Bey, I., Fiore, A. M., Li, Q., Yantosca, R. M., and Koelemeijer, R. B. A.: An improved retrieval of tropospheric nitrogen dioxide from GOME, *J. Geophys. Res.*, 107(D20), 4437, doi:10.1029/2001JD001027, 2002.

**Aerosol impact on
the NO₂ airmass
factor**

J. Leitão et al.

[Title Page](#)[Abstract](#)[Introduction](#)[Conclusions](#)[References](#)[Tables](#)[Figures](#)[◀](#)[▶](#)[◀](#)[▶](#)[Back](#)[Close](#)[Full Screen / Esc](#)[Printer-friendly Version](#)[Interactive Discussion](#)

Martin, R. V., Jacob, D. J., Chance, K., Kurosu, T. P., Palmer, P. I., and Evans, M. J.: Global inventory of nitrogen oxide emissions constrained by space-based observations of NO₂ columns, *J. Geophys. Res.*, 108(D17), 4537, doi:10.1029/2003JD003453, 2003.

Mattis, I., Ansmann, A., Müller, D., Wandinger, U., and Althausen, D.: Dual-wavelength Raman lidar observations of the extinction-to-backscatter ratio of Saharan dust, *Geophys. Res. Lett.*, 29(9), 1306, doi:10.1029/2002GL014721, 2002.

Mattis, I., Ansmann, A., Müller, D., Wandinger, U., and Althausen, D.: Multiyear aerosol observations with dual-wavelength Raman lidar in the framework of EARLINET, *J. Geophys. Res.*, 109, D13203, doi:10.1029/2004JD004600, 2004.

Mishchenko FORTRAN codes: <http://www.giss.nasa.gov/staff/mmishchenko/brf/>, last access: October 2009, 2008.

Müller, D., Mattis, I., Wandinger, U., Ansmann, A., Althausen, D., Dubovik, O., Eckhardt, S., and Stohl, A.: Saharan dust over a central European EARLINET-AERONET site: Combined observations with Raman lidar and Sun photometer, *J. Geophys. Res.*, 108(D12), 4345, doi:10.1029/2002JD002918, 2003.

Müller, D., Mattis, I., Wandinger, U., Ansmann, A., Althausen, D., and Stohl, A.: Raman lidar observations of aged Siberian and Canadian forest fire smoke in the free troposphere over Germany in 2003: Microphysical particle characterization, *J. Geophys. Res.*, 110, D17201, doi:10.1029/2004JD005756, 2005.

Murayama, T., Sugimoto, N., Uno, I., Kinoshita, K., Aoki, K., Hagiwara, N., Liu, Z., Matsui, I., Sakai, T., Shibata, T., Arao, K., Sohn, B.-J., Won, J.-G., Yoon, S.-Y., Li, T., Zhou, J., Hu, H., Abo, M., Iokibe, K., Koga, R., and Iwasaka, Y.: Ground-based network observation of Asian dust events of April 1998 in East Asia, *J. Geophys. Res.*, 106(D16), 18345–18359, 2001.

Murayama, T., Masonis, S. J., Redemann, J., Anderson, T. L., Schmid, B., Livingston, J. M., Russell, P. B., Huebert, B., Howell, S. G., McNaughton, C. S., Clarke, A., Abo, M., Shimizu, A., Sugimoto, N., Yabuki, M., Kuze, H., Fukagawa, S., Maxwell-Meier, K., Weber, R. J., Orsini, D. A., Blomquist, B., Bandy, A., and Thornton, D.: An intercomparison of lidar-derived aerosol optical properties with airborne measurements near Tokyo during ACE-Asia, *J. Geophys. Res.*, 108(D23), 8651, doi:10.1029/2002JD003259, 2003.

Murayama, T., Müller, D., Wada, K., Shimizu, A., Sekiguchi, M., and Tsukamoto, T.: Characterization of Asian dust and Siberian smoke with multi-wavelength Raman lidar over Tokyo, Japan in spring 2003, *Geophys. Res. Lett.*, 31, L23103, doi:10.1029/2004GL021105, 2004.

- Nüß, J. H.: Verbesserungen des troposphärischen NO₂-Retrievals aus GOME- und SCIAMACHY-Daten, Ph.D. thesis, Bremen University, Bremen, 2005.
- Papayannis, A., Amiridis, V., Mona, L., Tsaknakis, G., Balis, D., Bösenberg, J., Chaikovski, A., De Tomasi, F., Grigorov, I., Mattis, I., Mitev, V., Müller, D., Nickovic, S., Pérez, C., Pietruczuk, A., Pisani, G., Ravetta, F., Rizi, V., Sicard, M., Trickl, T., Wiegner, M., Gerd-
5 ing, M., Mamouri, R. E., D'Amico, G., and Pappalardo, G.: Systematic lidar observations of Saharan dust over Europe in the frame of EARLINET (2000–2002), *J. Geophys. Res.*, 113, D10204, doi:10.1029/2007JD009028, 2008.
- Pérez, C., Nickovic, S., Baldasano, J. M., Sicard, M., Rocadenbosch, F., and Cachorro, V. E.: A
10 long Saharan dust event over the western Mediterranean: lidar, sunphotometer observations, and regional dust modeling, *J. Geophys. Res.*, 111, D15214, doi:10.1029/2005JD006579, 2006.
- Platt, U. and Stutz, J.: Differential Optical Absorption Spectroscopy: Principles and Applications, in: *Physics of Earth and Space Environments*, Springer, Berlin, 2008.
- 15 Richter, A. and Burrows, J. P.: Tropospheric NO₂ from GOME measurements, *Adv. Space Res.*, 29(11), 1673–1683, 2002.
- Richter, A., Burrows, J. P., Nüß, H., Granier, C., and Niemeier, U.: Increase in tropospheric nitrogen dioxide over China observed from space, *Nature*, 437, 129–132, 2005.
- Rozanov, A., Rozanov, V., Buchwitz, M., Kokhanovsky, A., and Burrows, J. P.: SCIATRAN 2.0
20 – A new radiative transfer model for geophysical applications in the 175–2400 nm spectral region, *Adv. Space Res.*, 36(5), 1015–1019, doi:10.1016/j.asr.2005.03.012, 2005.
- Schmidt, H., Derognat, C., Vautard, R., and Beekmann, M.: A comparison of simulated and observed ozone mixing ratios for summer of 1998 in western Europe, *Atmos. Environ.*, 35, 6277–6297, 2001.
- 25 Seinfeld, J. H. and Pandis, S. N.: *Atmospheric Chemistry and Physics: From Air Pollution to Climate Change*, John Wiley & Sons, New York, 1998.
- Solomon, S., Schmeltekopf, A. L., and Sanders, R. W.: On the interpretation of zenith sky absorption measurements, *J. Geophys. Res.*, 92(D7), 8311–8319, 1987.
- Solomon, S., Portmann, W., Sanders, R. W., Daniel, J. S., Madsen, W., Bartram, B., and Dutton,
30 E. G.: On the role of nitrogen dioxide in the absorption of solar radiation, *J. Geophys. Res.*, 104(D10), 12047–12058, 1999.

**Aerosol impact on
the NO₂ airmass
factor**J. Leitão et al.

[Title Page](#)[Abstract](#)[Introduction](#)[Conclusions](#)[References](#)[Tables](#)[Figures](#)[◀](#)[▶](#)[◀](#)[▶](#)[Back](#)[Close](#)[Full Screen / Esc](#)[Printer-friendly Version](#)[Interactive Discussion](#)

- Thomas, W., Erbertseder, T., Ruppert, T., van Roozendael, M., Verdebout, J., Balis, D., Meleti C., and Zerefos, C.: On the retrieval of volcanic sulfur dioxide emissions from GOME backscatter measurements, *J. Atmos. Chem.*, 50, 295–320, doi:10.1007/s10874-005-5544-1, 2005.
- van der A, R. J., Eskes, H. J., Boersma, K. F., van Noije, T. P. C., van Roozendael, M., de Smedt, I., Peters, D. H. M. U., and Meijer, E. W.: Trends, seasonal variability and dominant NO_x source derived from a ten year record of NO₂ measured from space, *J. Geophys. Res.*, 113, D04302, doi:10.1029/2007JD009021, 2008.
- Vasilkov, A. P., Joiner, J., Oreopoulos, L., Gleason, J. F., Veeffkind, P., Bucselá, E., Celarier, E. A., Spurr, R. J. D., and Platnick, S.: Impact of tropospheric nitrogen dioxide on the regional radiation budget, *Atmos. Chem. Phys.*, 9, 6389–6400, 2009, <http://www.atmos-chem-phys.net/9/6389/2009/>.
- Wang, K., Dickinson, R. E., and Liang, S.: Clear sky visibility has decreased over land globally from 1973 to 2007, *Science*, 323, 1468–1470, 2009.
- Winker, D. M., Pelon, J. R., and McCormick, M. P.: The CALIPSO mission: Spaceborne lidar for observation of aerosols and clouds, in: *Proceedings of the Lidar Remote Sensing for Industry and Environment Monitoring III Conference*, Hangzhou, China, 24 October 2002, 4893, 1–11, 2003.
- Zhang, Q., Streets, D. G., He, K., Wang, Y., Richter, A., Burrows, J. P., Uno, I., Jang, C. J., Chen, D., Yao, Z., and Lei, Y.: NO_x emission trends for China, 1995–2004: The view from the ground and the view from space, *J. Geophys. Res.*, 112, D22306, doi:10.1029/2007JD008684, 2007.
- Zhou, J., Yu, G., Jin, C., Qi, F., Liu, D., Hu, H., Gong, Z., Shi, G., Nakajima, T., and Takamura, T.: Lidar observations of Asian dust over Hefei, China, in spring 2000, *J. Geophys. Res.*, 107(D15), 4252, doi:10.1029/2001JD000802, 2002.

**Aerosol impact on
the NO₂ airmass
factor**J. Leitão et al.

[Title Page](#)[Abstract](#)[Introduction](#)[Conclusions](#)[References](#)[Tables](#)[Figures](#)[⏪](#)[⏩](#)[◀](#)[▶](#)[Back](#)[Close](#)[Full Screen / Esc](#)[Printer-friendly Version](#)[Interactive Discussion](#)

Aerosol impact on the NO₂ air mass factor

J. Leitão et al.

Table 1. Scenarios considered for the SCIATRAN runs, defined by the combination of a NO₂ and an aerosol layer, as in box profiles (e.g. Scen. B: NO₂ layer 0–1.0 km and aerosol layer 0–0.6 km).

Scenario	A	B	C	D	E	F	G	H
NO ₂ layer (km)	0–0.6	0–1.0			0–2.0			0–2.0
Aerosol layer (km)	0–0.6	0–0.6	0–1.0	0.6–1.0	1.0–2.0	0–2.0	2.0–3.0	0–2.0

Title Page

Abstract

Introduction

Conclusions

References

Tables

Figures

⏪

⏩

◀

▶

Back

Close

Full Screen / Esc

Printer-friendly Version

Interactive Discussion



Aerosol impact on the NO₂ air mass factor

J. Leitão et al.

Title Page

Abstract

Introduction

Conclusions

References

Tables

Figures

◀

▶

◀

▶

Back

Close

Full Screen / Esc

Printer-friendly Version

Interactive Discussion



Table 2. Aerosol parameters (single scattering albedo (ω_0), Ångström exponent (α) and aerosol optical depth (AOD)) taken from each of the references mentioned that were used to define the aerosol vertical profile (with extinction coefficients) for the SCIATRAN scenarios. These are representative of different aerosol types: Urban (Urb), Desert Dust (DD), and biomass burning (BB) scenes.

Scenario and Reference for aerosol ext. profile	Aerosol type	ω_0	α	AOD	Further notes
I based on CALIPSO records ^a	Urb	0.93 ^b	1.4 ^c	0.07	Background conditions
J Chazette et al. (2005)	Urb	0.87	2.1	0.40	19 July 2000 in Paris (FR)
K Amiridis et al. (2005)	Urb	0.93 ^b	1.4 ^c	0.62	4 yr average over Thessaloniki (GR)
L Zhou et al. (2002)	DD	0.92 ^b	0.19	1.05	12 May 2000 in Heifei (CN)
M Murayama et al. (2003)	DD	Altitude dependent values – 0.8 to 0.95	Altitude dependent values – 0.01 to 1.1	0.66	23 April 2001 in Tokyo (JP)
N Pérez et al. (2006)	DD	0.93	0.19 ^d	0.16	18 June 2003 in Barcelona (SP)
O Balis et al. (2003)	BB	0.92 ^b	1.4 ^e	1.05	9 August 2001 in Thessaloniki (GR)
P Müller et al. (2005)	BB	0.92 ^b	Altitude dependent values – 0 to 1.1	0.42	26 June 2003 in Leipzig (DE)

^a Data provided by Chieko Kittaka and David Winker from NASA – Goddard Space Flight Center.

^b Average of the respective aerosol type based on Dubovik et al. (2002).

^c Average for urban aerosol in Mattis et al. (2004).

^d Same as Zhou et al. (2002).

^e From Müller et al. (2005) and references therein.

**Aerosol impact on
the NO₂ air mass
factor**

J. Leitão et al.

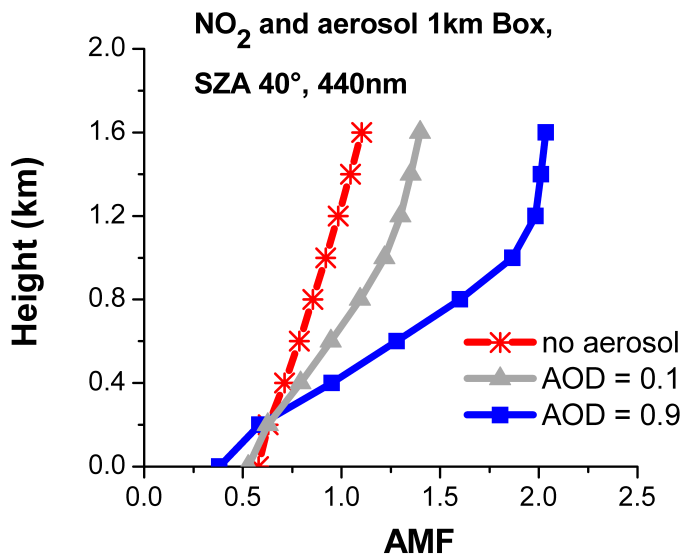


Fig. 1. NO₂ air mass factor vertical variation for 3 scenarios: no aerosol (red), and an aerosol layer with SSA of 0.93 extending from the surface to 1.0 km with an optical depth (AOD) of 0.1 (grey) and 0.9 (blue). AMFs determined at 440 nm, with surface albedo = 0.03, $\omega_0=0.93$ and solar zenith angle (SZA) of 40°.

[Title Page](#)[Abstract](#)[Introduction](#)[Conclusions](#)[References](#)[Tables](#)[Figures](#)[◀](#)[▶](#)[◀](#)[▶](#)[Back](#)[Close](#)[Full Screen / Esc](#)[Printer-friendly Version](#)[Interactive Discussion](#)

**Aerosol impact on
the NO₂ airmass
factor**

J. Leitão et al.

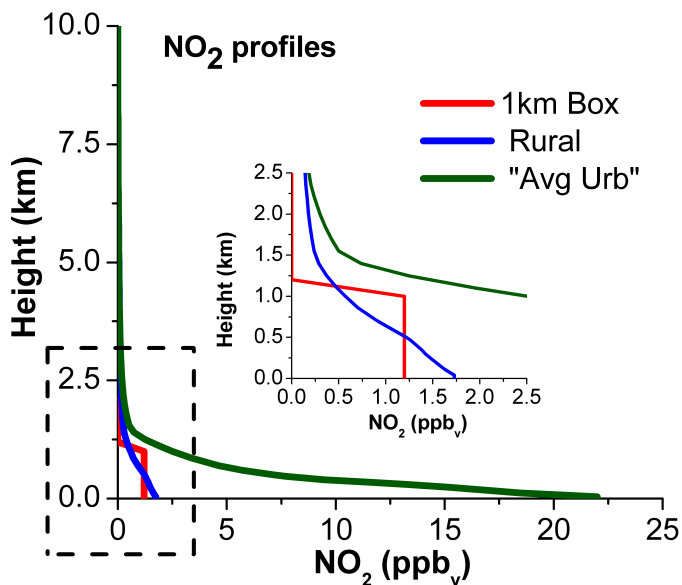


Fig. 2. NO₂ profiles from surface to 10.0 km used in the SCIATRAN settings for the airmass calculations: (red) box profile of 1.0 km; (green) average urban ("Avg Urb") and (blue) rural are based on CHIMERE model results.

[Title Page](#)[Abstract](#)[Introduction](#)[Conclusions](#)[References](#)[Tables](#)[Figures](#)[◀](#)[▶](#)[◀](#)[▶](#)[Back](#)[Close](#)[Full Screen / Esc](#)[Printer-friendly Version](#)[Interactive Discussion](#)

**Aerosol impact on
the NO₂ airmass
factor**

J. Leitão et al.

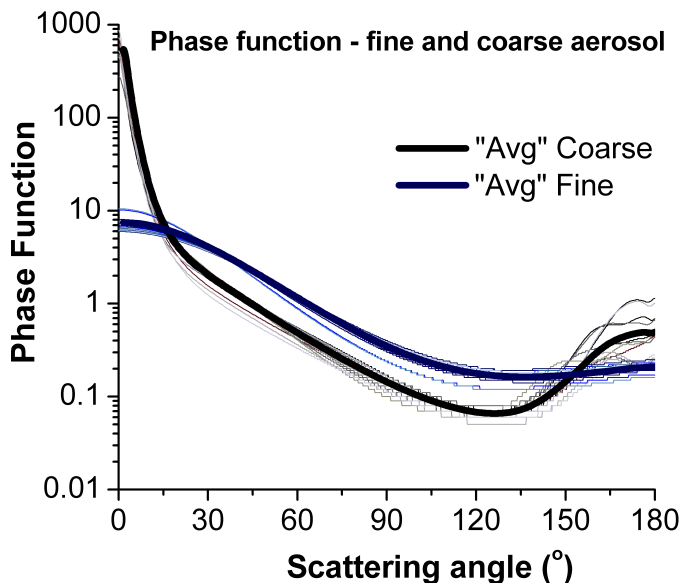


Fig. 3. Phase functions at 440 nm for fine (blue) and coarse (grey) aerosol determined for 4 distinct aerosol types: Urban (Urb), Biomass Burning (BB), Desert Dust (DD) and Oceanic. Optical properties taken from 12 AERONET stations: Paris/Creteil – France (Urb), GSFC/Maryland – USA (Urb), Maldives (Urb), Mexico city – Mexico (Urb), Amazonia forest – Brazil (BB), South American cerrado – Brazil (BB), African savanna – Zambia (BB), Boreal forest – USA and Canada (BB), Cape Verde (DD), Persian Gulf (DD), Saudi Arabia (DD) and Lanai (Oceanic). Average of phase functions for each of the aerosol sizes considered is presented in thick lines (blue for fine and black for coarse aerosol).

[Title Page](#)[Abstract](#)[Introduction](#)[Conclusions](#)[References](#)[Tables](#)[Figures](#)[◀](#)[▶](#)[◀](#)[▶](#)[Back](#)[Close](#)[Full Screen / Esc](#)[Printer-friendly Version](#)[Interactive Discussion](#)

**Aerosol impact on
the NO₂ airmass
factor**

J. Leitão et al.

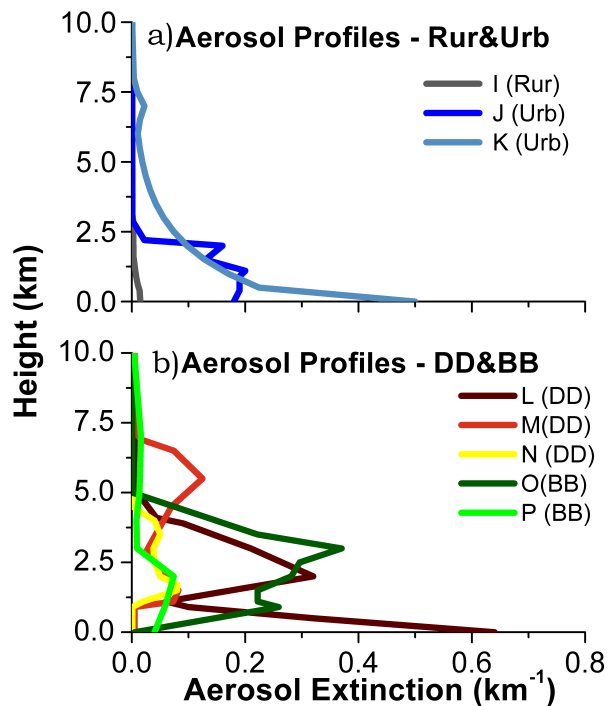


Fig. 4. Aerosol extinction profiles from surface level to 10 km used in the SCIATRAN settings for the airmass factor calculations for: **(a)** Rural (Rur) and urban (Urb) locations; and **(b)** desert dust (DD) events and biomass burning (BB) plumes. These profiles are based on measurements performed in different locations as it is explained in Table 2.

[Title Page](#)[Abstract](#)[Introduction](#)[Conclusions](#)[References](#)[Tables](#)[Figures](#)[◀](#)[▶](#)[◀](#)[▶](#)[Back](#)[Close](#)[Full Screen / Esc](#)[Printer-friendly Version](#)[Interactive Discussion](#)

Aerosol impact on
the NO_2 airmass
factor

J. Leitão et al.

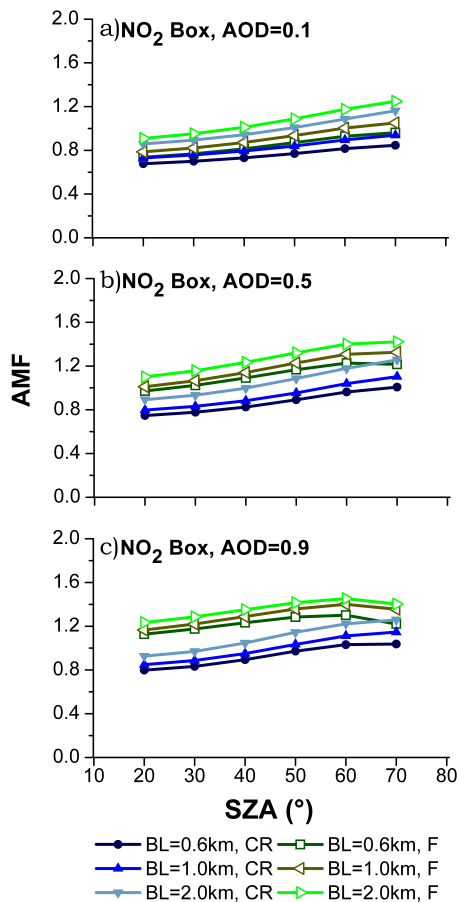


Fig. 5. NO_2 airmass factors for scenarios A, C and H (well mixed NO_2 and aerosol layers extending to: 0.6, 1.0 and 2.0 km, respectively) calculated with the phase functions determined for coarse (CR) and fine (F) particles (optical properties taken from Creteil/Paris AERONET station). AMFs determined at 440 nm, with surface albedo = 0.03, $\omega_0=0.93$ and different AODs: **(a)** 0.1, **(b)** 0.5 and **(c)** 0.9.

[Title Page](#)[Abstract](#)[Introduction](#)[Conclusions](#)[References](#)[Tables](#)[Figures](#)[◀](#)[▶](#)[◀](#)[▶](#)[Back](#)[Close](#)[Full Screen / Esc](#)[Printer-friendly Version](#)[Interactive Discussion](#)

Aerosol impact on the NO₂ airmass factor

J. Leitão et al.

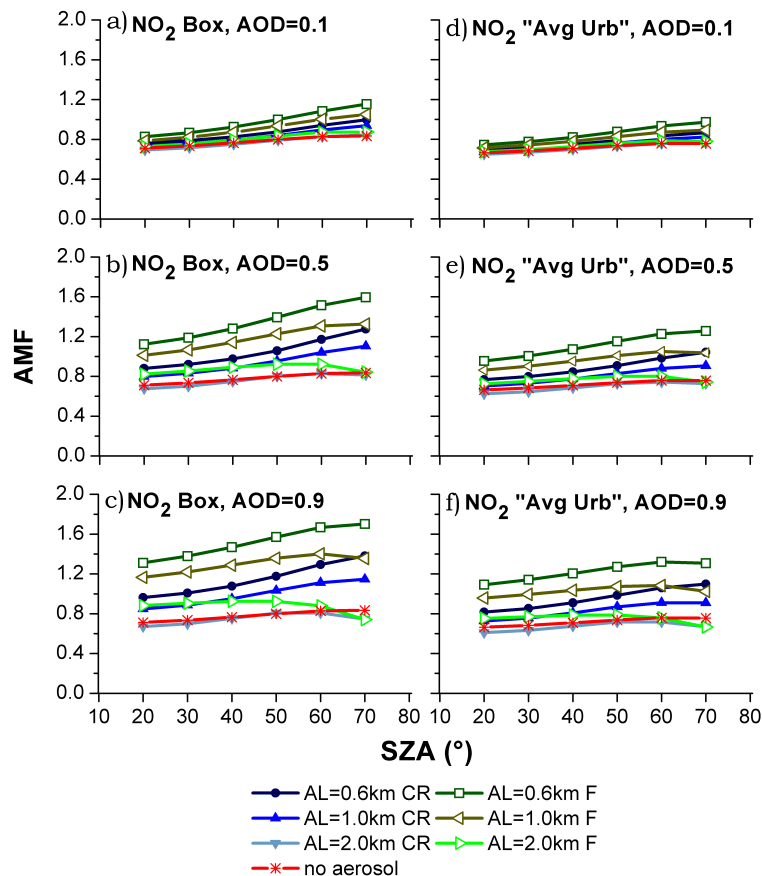


Fig. 6. (a–c) NO₂ airmass factors for a 1.0 km box NO₂ profile using no aerosol (red) and for the scenarios B, C and F (extension of aerosol layer (AL) from surface to 0.6, 1.0 and 2.0 km, respectively) calculated with the phase functions determined for coarse (CR) and fine (F) particles (optical properties taken from Creteil/Paris AERONET station). AMFs determined at 440 nm, with surface albedo = 0.03, $\omega_0=0.93$ and different AOD: (top) 0.1, (middle) 0.5, (bottom) 0.9. (d–e) Same as (a–c) for the aerosol settings but using the average of modelled urban NO₂ profile ("Avg Urb").

Title Page

Abstract

Introduction

Conclusions

References

Tables

Figures

◀

▶

◀

▶

Back

Close

Full Screen / Esc

Printer-friendly Version

Interactive Discussion



Aerosol impact on the NO₂ air mass factor

J. Leitão et al.

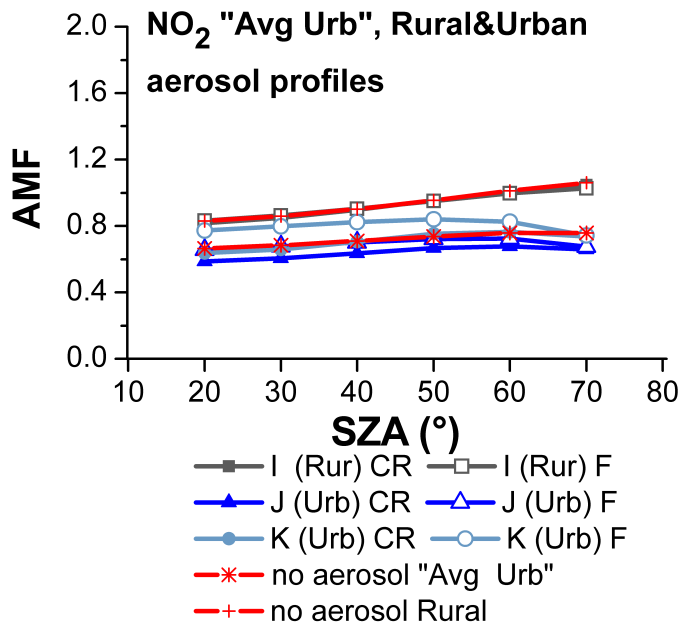


Fig. 7. NO₂ air mass factors for no aerosol (red) cases (rural and urban NO₂ profiles from CHIMERE) and for the scenarios I (background – Rur – NO₂ and aerosol vertical profiles), J and K (urban – Urb – NO₂ and aerosol vertical profiles) calculated with the phase functions determined for coarse (CR) and fine (F) particles (optical properties taken from Creteil/Paris AERONET station). AMFs determined at 440 nm, with surface albedo = 0.03, and ω_0 and AOD defined according to the measurements (see Table 2).

Title Page

Abstract

Introduction

Conclusions

References

Tables

Figures

◀

▶

◀

▶

Back

Close

Full Screen / Esc

Printer-friendly Version

Interactive Discussion



Aerosol impact on the NO₂ airmass factor

J. Leitão et al.

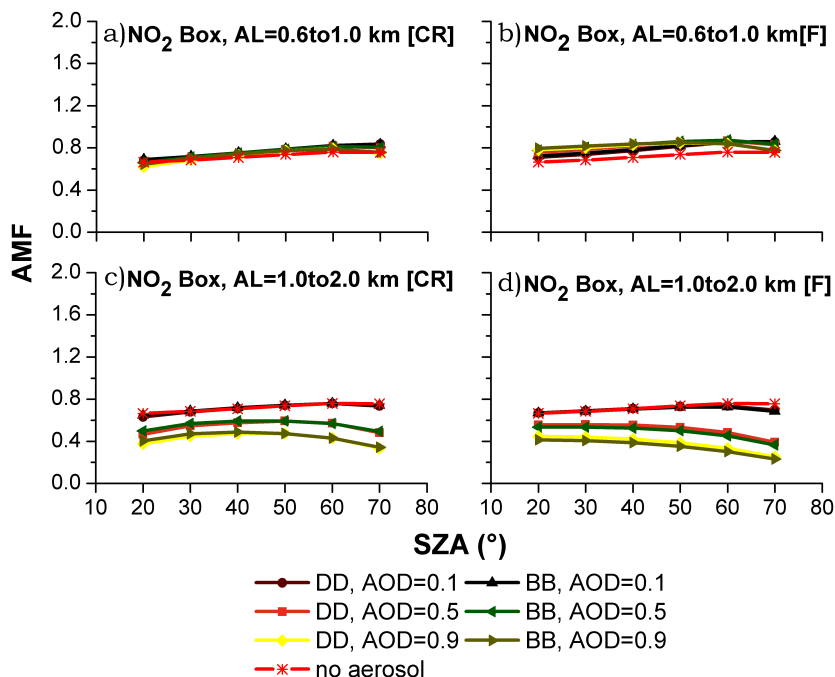


Fig. 8. NO₂ airmass factors for a 1.0 km box NO₂ profile using no aerosol (red) and also for scenarios D (a, b) and E (c, d) (elevated aerosol layers (AL) from 0.6 to 1.0 km and 1.0 to 2.0 km, respectively) calculated with the phase functions determined for coarse (a, c) and fine (b, d) particles (optical properties taken from Amazonia forest/Brazil and from Saudi Arabia AERONET stations respectively for the biomass burning (BB) and desert dust (DD) cases). AMF determined at 440 nm, with surface albedo = 0.03, $\omega_0 = 0.93$ and different AOD: 0.1, 0.5, and 0.9.

Title Page

Abstract

Introduction

Conclusions

References

Tables

Figures

◀

▶

◀

▶

Back

Close

Full Screen / Esc

Printer-friendly Version

Interactive Discussion



**Aerosol impact on
the NO₂ airmass
factor**

J. Leitão et al.

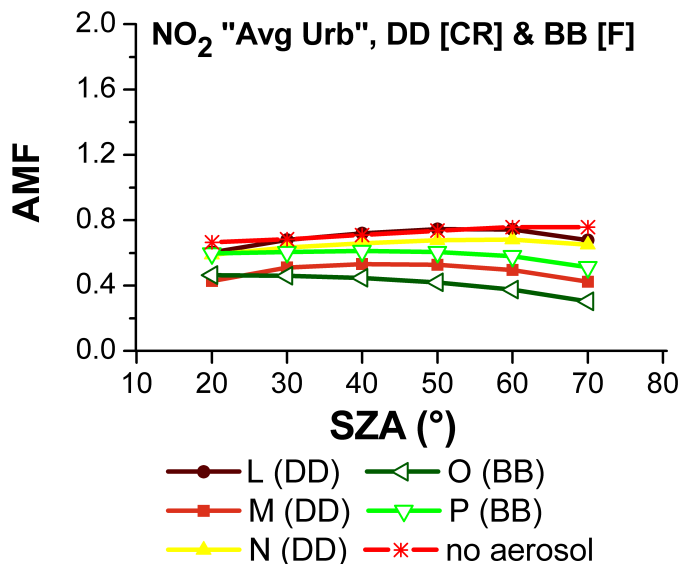


Fig. 9. NO₂ airmass factors for urban NO₂ profile from CHIMERE using no aerosol and also for scenarios L to P (measured aerosol profiles) calculated with the phase functions determined for desert dust (DD) coarse (CR) particles (optical properties taken from Saudi Arabia AERONET station) and for biomass burning (BB) fine (F) particles (optical properties taken from Amazonia forest/Brazil AERONET station). AMFs determined at 440 nm, with surface albedo = 0.03, and ω_0 and AOD defined according to the measurements (see Table 2).

Title Page

Abstract

Introduction

Conclusions

References

Tables

Figures

◀

▶

◀

▶

Back

Close

Full Screen / Esc

Printer-friendly Version

Interactive Discussion



Aerosol impact on the NO₂ air mass factor

J. Leitão et al.

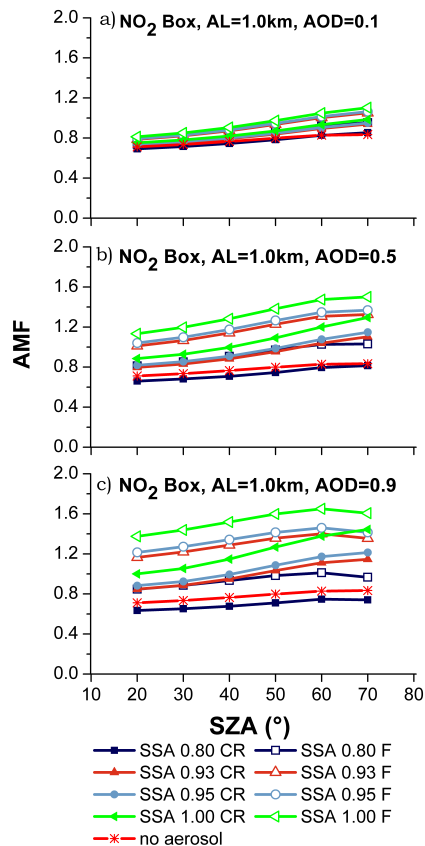


Fig. 10. NO₂ air mass factors for simulations with different single scattering albedo (SSA) for scenario C (NO₂ and aerosol layer (AL) – 1.0 km box profile) calculated with the phase functions determined for coarse (CR) and fine (F) particles (optical properties taken from Creteil/Paris AERONET station). AMFs determined at 440 nm, with surface albedo = 0.03, and different AODs: (a) 0.1, (b) 0.5 and (c) 0.9.

Title Page

Abstract

Introduction

Conclusions

References

Tables

Figures

◀

▶

◀

▶

Back

Close

Full Screen / Esc

Printer-friendly Version

Interactive Discussion



Aerosol impact on the NO₂ airmass factor

J. Leitão et al.

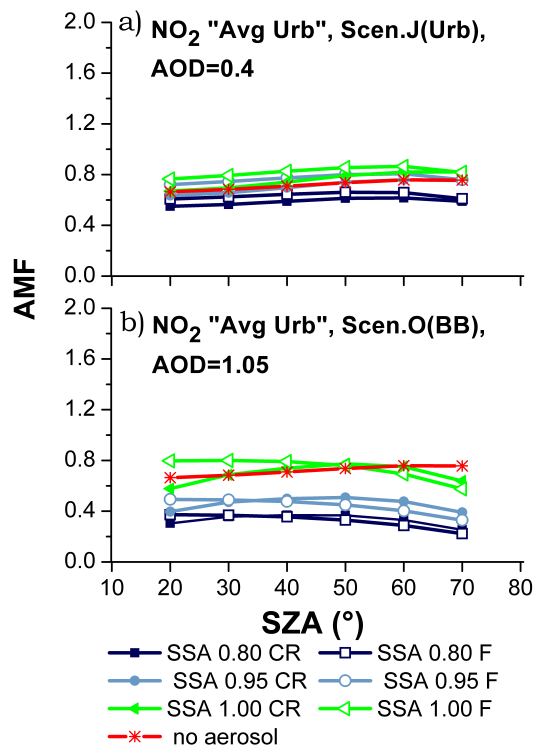


Fig. 11. NO₂ airmass factors for different single scattering albedo (SSA) for scenario **(a)** J and **(b)** O (urban NO₂ profile from CHIMERE with urban and biomass burning aerosol, respectively) calculated with the phase functions determined for coarse (CR) and fine (F) particles (optical properties taken from Creteil/Paris and Amazonia forest/Brazil AERONET stations for scenario J and O, respectively). AMFs determined at 440 nm, with surface albedo = 0.03, and the AOD defined according to the measurements.

Title Page

Abstract

Introduction

Conclusions

References

Tables

Figures

◀

▶

◀

▶

Back

Close

Full Screen / Esc

Printer-friendly Version

Interactive Discussion

